

Evaluation of Flood Evacuation Possibility under the Global Warming Condition in Kakehashi River Basin based on Inundation Simulation

Noriyasu Nakade^{1*}, Kenji Taniguchi²

¹ Graduate School of Natural Science and Technology, Kanazawa University
Kakuma-machi, Kanazawa, Ishikawa, 920-1192, JAPAN

² Faculty of Geoscience and Civil Engineering, Kanazawa University
Kakuma-machi, Kanazawa, Ishikawa, 920-1192, JAPAN

*E-mail: noriyasu.nakade@toyosk.co.jp

Abstract: As for the arrival time of the flooding stream in the flood inundation assumption area, it varies by the topography and the distance from the river. For example, there are higher risk of inundation by overflow and erosion of river bank along the riverside, and the arrival time of flood is shorter than other areas. Then, earlier evacuation is needed. On the other hand, in the flood management plan, the single lead time for evacuation (or time required for evacuation) is uniformly decided for one targeted basin. In the case of Kanto-Tohoku heavy rainfall in September 2015, wide areas of the basin were inundated by dyke break, and many people delayed evacuation and stood alone. In flood management under the changing climate, not only structural measures, but secure evacuation remains an important issue. In Kakehashi river flowing through Komatsu City (the second largest city in Ishikawa, Japan), the record maximum water level was observed at the heavy rainfall in 2013. In this study, reproductive and future simulations of the heavy rainfall in 2013 were implemented by using a numerical weather model. For future simulations, the pseudo global warming (PGW) method was applied using future projections by multiple global climate models. At the same time, an ensemble simulation technique was combined with PGW method to consider uncertainty of climate change. Based on multiple rainfall patterns from the weather simulation results, runoff analyses were made for the Kakehashi river basin. Then, high spatial resolution (40m x 40m) inundation simulations were implemented. Using the inundation simulation results, expected arrival times of flood were estimated for each grid in the target area and the possibilities of evacuation were compared for different rainfall patterns.

Keywords: flood, evacuation, global warming, inundation simulation

1. Introduction

In 2018, there was a record heavy rainfall in the

western part of Japan. Because of flood inundation caused by dyke break of Oda river and its branch,

there were 51 death toll at Mabi-town in Kurashiki City. Many of the victims were elderly people over 70. Their houses were not swept away by flood, but it was difficult for them to evacuate upstairs. It is pointed out that “delayed escape” was main cause to become victims. In September 2015, 4,300 people were delayed to escape and isolated in the case of flood disaster occurred in Kanto area, Japan. Then, information services have been improved to realize early evacuation in cases of water-related disasters. However, many people remained their house and delayed to escape in the 2018 flood event.

In Japan, river administrators provide information of risks by water-related disasters: the maximum inundation depth, duration of inundation, and presence or absence of collapse of houses. Such information indicates the worst conditions or final state of disaster, but not temporal progress of flood inundation. So it is difficult to understand imminently dangerous situations. In addition, there is concerns of more frequent and intense heavy rainfall in future climate caused by global warming, and it is important to consider their impact on disaster prevention planning.

In Kakehashi river flowing through Komatsu City (the second largest city in Ishikawa prefecture, Japan), the record maximum water level was observed at the heavy rainfall in 2013. In this study, reproductive and future simulations of the heavy rainfall in 2013 were implemented by using a numerical weather model. At the same time, an ensemble simulation technique was combined with the pseudo global warming (PGW) method (Sato et al. 2007) to consider uncertainty of climate change. Based on multiple rainfall patterns from the weather simulation results, runoff analyses and inundation simulations were made for the Kakehashi river basin. Using the inundation simulation results, expected arrival times of flood were estimated for each grid in the target area and the potential time of evacuation

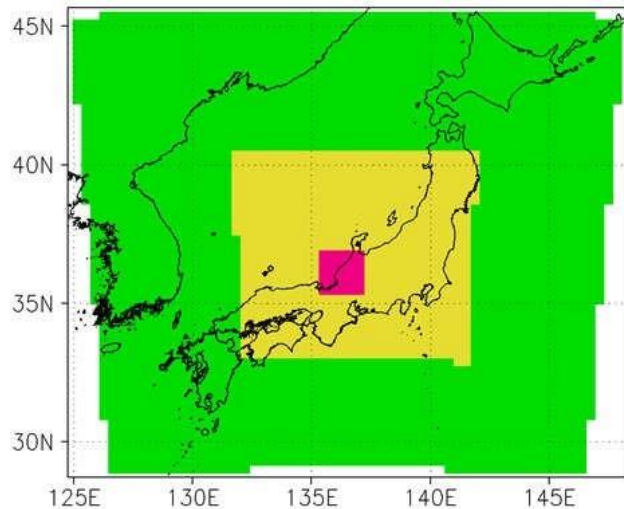


Figure 1 Areas for WRF simulation. Green, yellow and magenta indicate outer, intermediate, and inner domains, respectively.

Table 1 Settings for WRF

Items	Setting
Model Version	3.6.1
Spatial resolution	30km, 10km, 2km
Time interval	180 sec, 60 sec, 12sec
Microphysics	Lin Ice Scheme
Cumulus	Betts-Miller-Janjic
Radiation	Rapid Radiative Transfer Model
Surface layer physics	Monin-Obukov
Land surface	Noad Land Surface
Planetary boundary layer	Mellor-Yamada. Nakanishi and Niino Level 3 scheme
Data assimilation	Spectral nudging

(hereafter PTE) were compared for different rainfall patterns.

2. Methodology

2.1 Numerical weather simulation

2.1.1 Weather Research and Forecasting model

For numerical weather simulation, the Weather Research and Forecasting (WRF) version 3.6.1 (Skamarock et al. 2008) were used in this study. The WRF model is widely used for both operational

weather prediction and research activities. WRF is a non-hydrostatic model, which was developed to choose various dynamical and physical parameterizations. Settings for WRF is summarized in Table 1.

Simulation area for WRF simulation is shown in Fig. 1. The three-domain nesting method is applied with 30 km, 10 km, and 2 km horizontal grid resolutions for outer, intermediate, and inner domains, respectively.

For the initial and boundary conditions, downscaling simulations used JRA-55 (Kobayashi et al. 2016), NCEP-FNL (NCEP 2000), and NOAA OI SST (Reynolds et al. 2007) datasets.

2.1.2 Pseudo global warming method

For reproductive simulations of the heavy rainfall event in 2013 around Kakehashi river basin, initial and boundary conditions prepared from JRA-55, NCEP FNL, and NOAA 0.25 interpolated OI SST. Based on the reproductive simulation, future simulations of the heavy rainfall were implemented with pseudo global warming (PGW) forcing prepared by using future projections by the model for the coupled model inter-comparison project 5 (CMIP5, Taylor et al. 2012). PGW conditions were calculated from future and present climate conditions. The future weather conditions were obtained from the 10-year monthly mean from 2091 to 2100. Present climatic conditions were obtained from the 10-year monthly mean from 1996 to 2005. Then, anomalies of global warming were calculated as the difference between the future and present climatic conditions and added to JRA-55. Thus, a set of PGW conditions was constructed for the wind, atmospheric temperature, geopotential height, surface pressure, and specific humidity. For relative humidity, the original values in JRA-55 were retained in the PGW conditions, and specific humidity in these conditions was defined from the

relative humidity and the modified atmospheric temperature of the future climate. To prepare SST for the PGW condition, the SST anomaly obtained from future and present climate conditions in the CIMP5 output was added to the NOAA SST. In this study, future projections by CNRM-CM5 developed by National Centre for Meteorological Research in France, and HadGEM2-ES developed by UK Met Office. Future conditions under the RCP8.5 (Taylor et al. 2012) emission scenario were used in this study. In RCP8.5, the radiative forcing of the Earth become 8.5 W/m² larger than before the industrial revolution.

2.2 Runoff analysis and inundation simulation

This study, therefore, used the Rainfall-Runoff Inundation (RRI) model (Sayama et al. 2012), which is a fully coupled model of rainfall-runoff model and hydraulic inundation model. In RRI model, both slope and river are assumed within the same grid cell. The river channel is considered as a single line on the overlying slope cells. The 2-dimension diffusive wave model was adopted to calculate the flow over slope grid cells, while the 1-dimension diffusive wave model was applied for the main channel flow. For better representation of rainfall, runoff, and inundation processes, the surface and subsurface condition parameterization was enabled with vertical Green-Ampt model infiltration flow. Input data for RRI model was taken from the hydrological data and maps based on Shuttle Elevation Derivatives at multiple Scales (HydroSHEDS). Topography inputs of 15-arc second resolution (approximately 500m) for digital elevation model, flow accumulation, and flow direction was used for RRI model (Fig.2(a)). Results of numerical weather simulations were used as input for RRI model. In this study, two different rainfall patterns based on PGW condition by HadGEM2-ES and CNRM-CM5 were used for simulation.

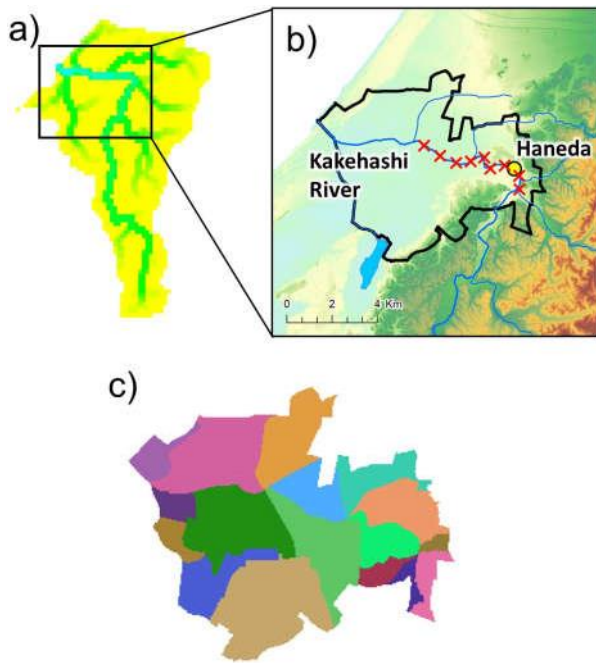


Figure 2 (a) Simulation area of RRI model, (b) Simulation area of inundation simulation (indicated by black line). Red crossed indicate sections of dyke break. (c) drainage districts for inundation simulations.

Inundation simulations were implemented by the seamlessly integrated model developed by the University of Tokyo (Sanuki et al., 2016). The model integrated 1-dimensional river model, surface flow model, and sewage network model. For Kakehashi river basin, sewage network data is not prepared and simple drainage model is developed. The target domain was separated into each drainage district and drainage capacity was provided (Fig.2c). Results of RRI model by two rainfalls were used in inundation simulations. In addition to upper and lower boundary of Kakehashi river, discharge of 5 branches were given as boundary conditions. Nine river sections were chosen to implement dyke-breaking simulations. Right and left bank was broken in simulation. Totally 18 dyke-breaking simulations were made for each flood wave (or RRI simulation by HadGEM2-ES and CNRM-CM5. In simulations, dyke break occurs when water level surpasses the high-water-level at each section. Width of dyke

break becomes huge from 25 m to 100 m in 1 hr.

2.3 Estimation of limit water level and time for evacuation

In this study, it is assumed that people need to evacuate when the maximum inundation depth is larger than 0.5m. Limitation inundation depths for evacuation, in which depth people cannot move, are decided for the cases of evacuation by car, and on foot, respectively. Then, the limit time of inundation on foot ($T_{L,F}$) and by car ($T_{L,C}$) are defined as follows.

$T_{L,F}$: arrival time of 0.1m immersion

$T_{L,C}$: arrival time of 0.3m immersion

Limit time for evacuation, or total window time for evacuation (T_{TE}) can be calculated as difference between $T_{L,F}$ (or $T_{L,C}$) and the time when the water level reaches the evacuation warning water level at the reference observatory. $T_{L,F}$ and $T_{L,C}$ were calculated to computational grids in which the maximum inundation depth is larger than 0.5m

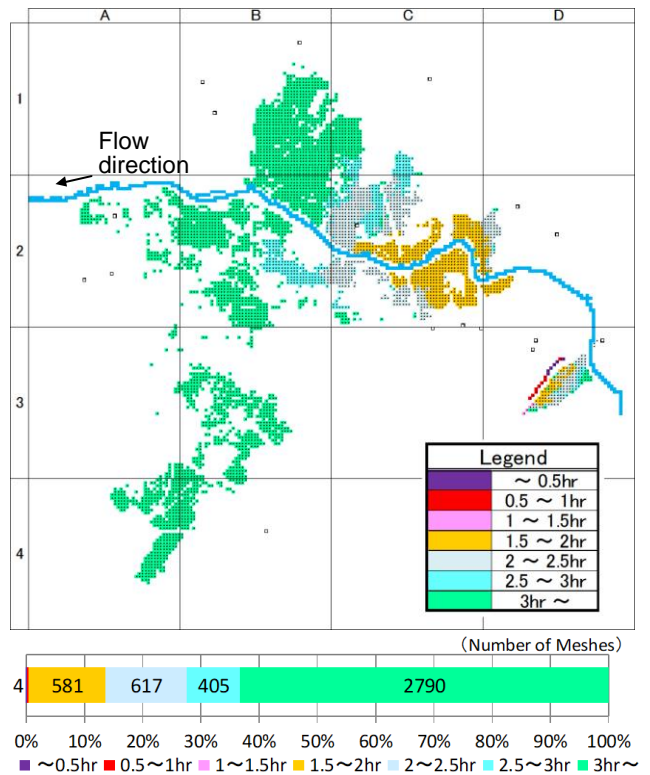


Figure 3 Spatial distribution of the total window time (T_{TE}) for evacuation estimated for evacuation on foot.

(where evacuation is necessary). Figure 3 shows spatial distribution of T_{TE} for the evacuation on foot. In the inundation area in upper and middle reach of Kakehashi river (areas C2, D2, and D3 in Fig.3), T_{TE} is shorter than 2.5 hrs. In the lower stream, T_{TE} is longer than 3 hrs. For the evacuation by car, there is no significant difference in T_{TE} .

2.4 Evaluation of possible time of evacuation

To reach the shelter safely, evacuation must be started at the appropriate time. Here, the window time between T_{TE} and the traveling time (T_{TR}) to the shelter is defined as potential time of evacuation (PTE). According to reference water levels, T_{TE} changes. In Japan, there are several reference water levels in rivers for disaster prevention. At the alert level 3, elderly adults and vulnerable people are recommended to evacuate. At the level 4, all people are expected to evacuate. Table 2 shows details of alert levels in Kakehashi river. The time when the water level reaches to these reference alert levels is defined as T_{AL} . Then, PTE is calculated by the following equation.

$$PTE = T_{L,*} - T_{AL} - T_{TR}$$

($T_{L,*}$ is $T_{L,F}$ or $T_{L,C}$)

Conditions to calculate T_{TR} are shown in Table 3. Details of estimate T_{AL} and T_{TR} are described below.

Table 2 Alert level for Kakehashi river

	Level 3	Level 4
Evacuation target	Elderly and vulnerable people	All people
Water Level (Kakehashi river)	7.15 m	7.55 m

Table 3 Condition of evacuation

		On foot	By car
Limit water		0.1 m	0.3 m
Travel speed	Level3 (Elderly and vulnerable)	38 m/min (2.3 km/h)	150 m/min (9.0 km/h)
	Level4 (All people)	60 m/min (3.6km/h)	

2.4.1 Estimation of alert water level time

Figure 4 shows a temporal variation of water level at Haneda (which is the reference observatory of Kakehashi river. See Fig.2b). Water level reaches to the alert level 3 and 4 at 20:51, and 21:34 on 28 July 2013, respectively. These times are used as T_{AL} to calculate PTE.

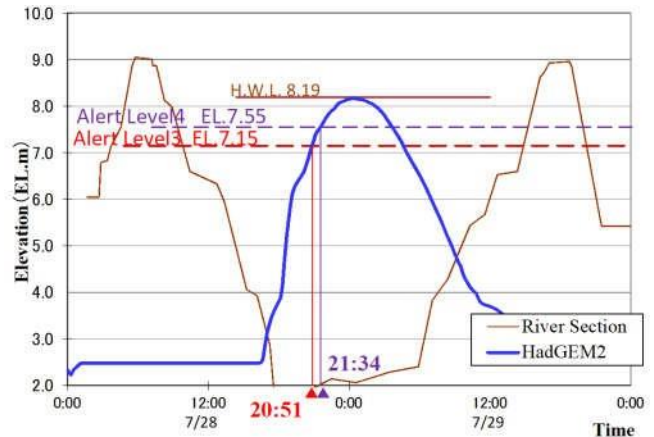


Figure 4 Temporal variation of water level at Haneda.

2.4.2 Traveling time to shelter

Traveling time to shelter (T_{TR}) from each computational grid to the nearest shelter are estimated.

First, the target area was separated to small blocks

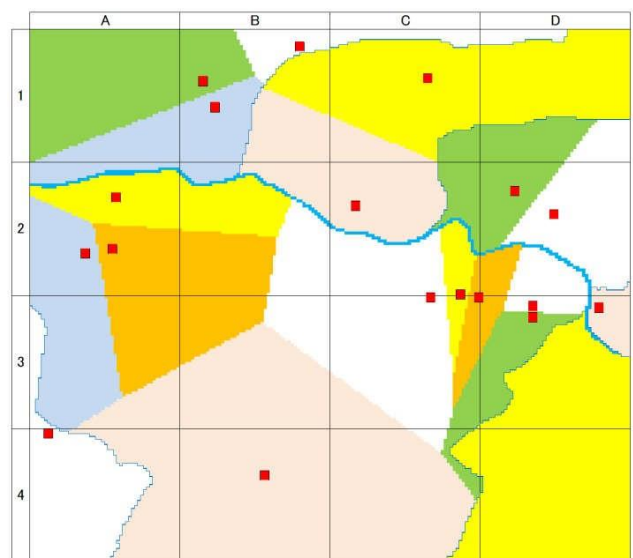


Figure 5 Locations of shelters and separation result of evacuation zone.

according to the location of shelters. The Thiessen method was applied in separation. In evacuation, people are assumed not to cross rivers. The result of area separation is shown in Fig. 5.

Next, path lengths to the nearest shelter from each computational grid are estimated. A path length is defined as $\sqrt{2} \times$ straight-line distance from a grid to the target shelter. Figure 6 shows spatial distribution of the path length to shelters. The path lengths are longer than 1 km in about 75 % of object grids.

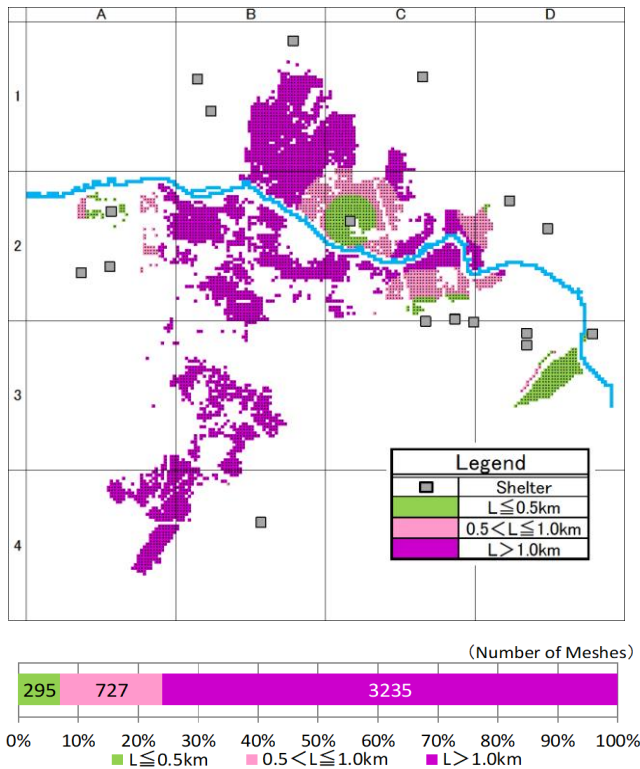


Figure 6 Path length from each computational grid to the nearest shelter.

Then, T_{TR} is calculated from the path lengths and travel speeds shown in Table 3. In the case of on-foot evacuation of elderly and vulnerable people, T_{TR} is longer than 30 min in 70 % of object grids (Fig.7a). In the case of ordinary people, T_{TR} is longer than 30 min in 45 % of object grids (Fig.7b). On the other hand, when using cars, T_{TR} is shorter than 20 min in the most of object grids (Fig.8).

3. Results of PTE estimation

Figure 9 shows PTE for the grid with the

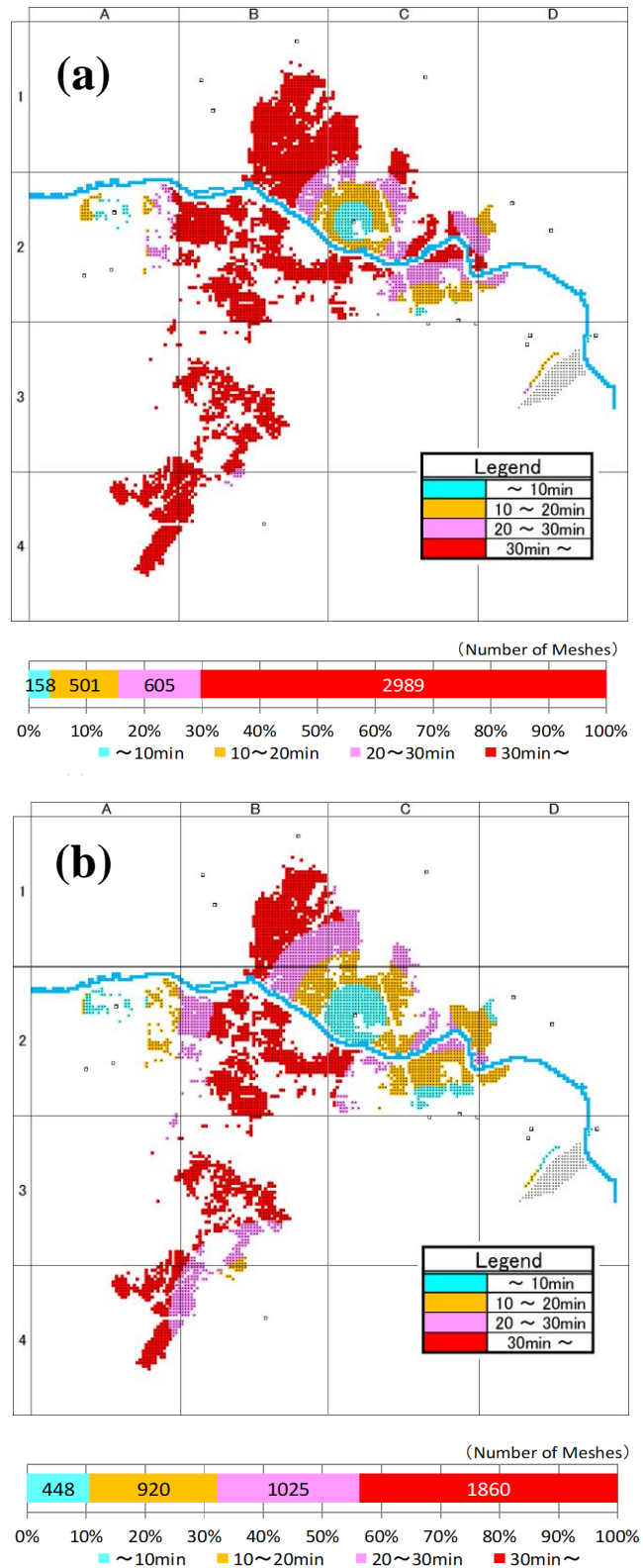


Figure 7 Travel time to the nearest shelter on foot (a) Elderly and vulnerable people. (b) Ordinary people.

maximum inundation depth > 0.5 m. The alert level 3 is applied to calculate PTE. Both in the cases of evacuation on foot and by car, PTE is short in B2

and C2 areas. Inundation flow arrives at these areas in early timing, and these areas are relatively far from shelters. Therefore, people in these areas should start evacuation in early timing. In the left bank of Kakehashi river around the boundary of B2 and C2 area, T_{TE} is 2-3 hrs and there is relatively long time to escape (Fig.9a). However, the shelter is far from this area and PTE is shorter than 2 hrs. On the other hand, in the lower stream areas, PTE is longer than 3 hrs. There is clear areal difference in PTE.

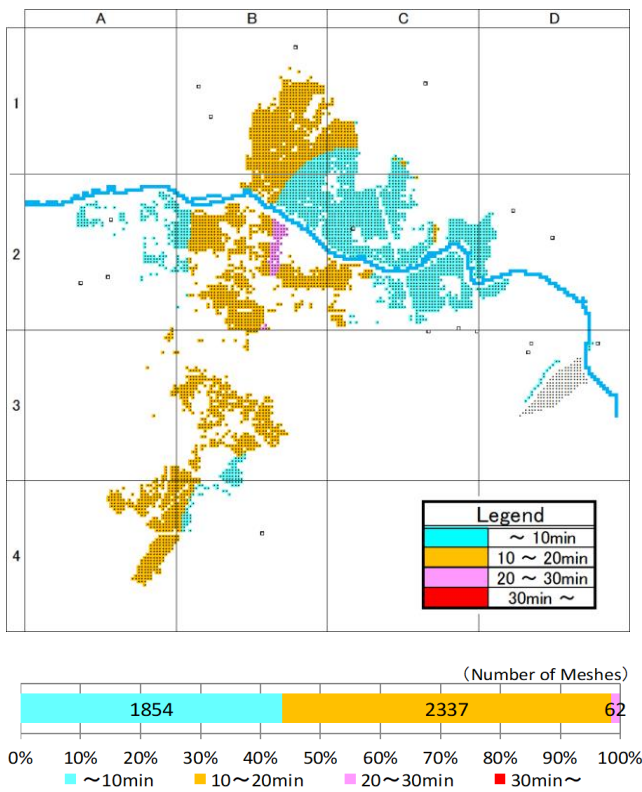


Figure 8 Travel time to the nearest shelter by car.

Figure 10a is frequency distribution of PTE. Frequency of $T_{TE} < 1.5$ hrs is small. However, considering T_{TR} , frequency of PTE < 1.5 significantly increases in the case of evacuation on foot. Cumulative distribution of PTE shows the window time of evacuation becomes 30 min shorter on foot. On the other hand, there is small difference between T_{TE} and PTE by car. Figure 10b is stacked chart of T_{TE} and PTE. As stated above, T_{TE} and PTE by car shows similar frequency distribution. On the

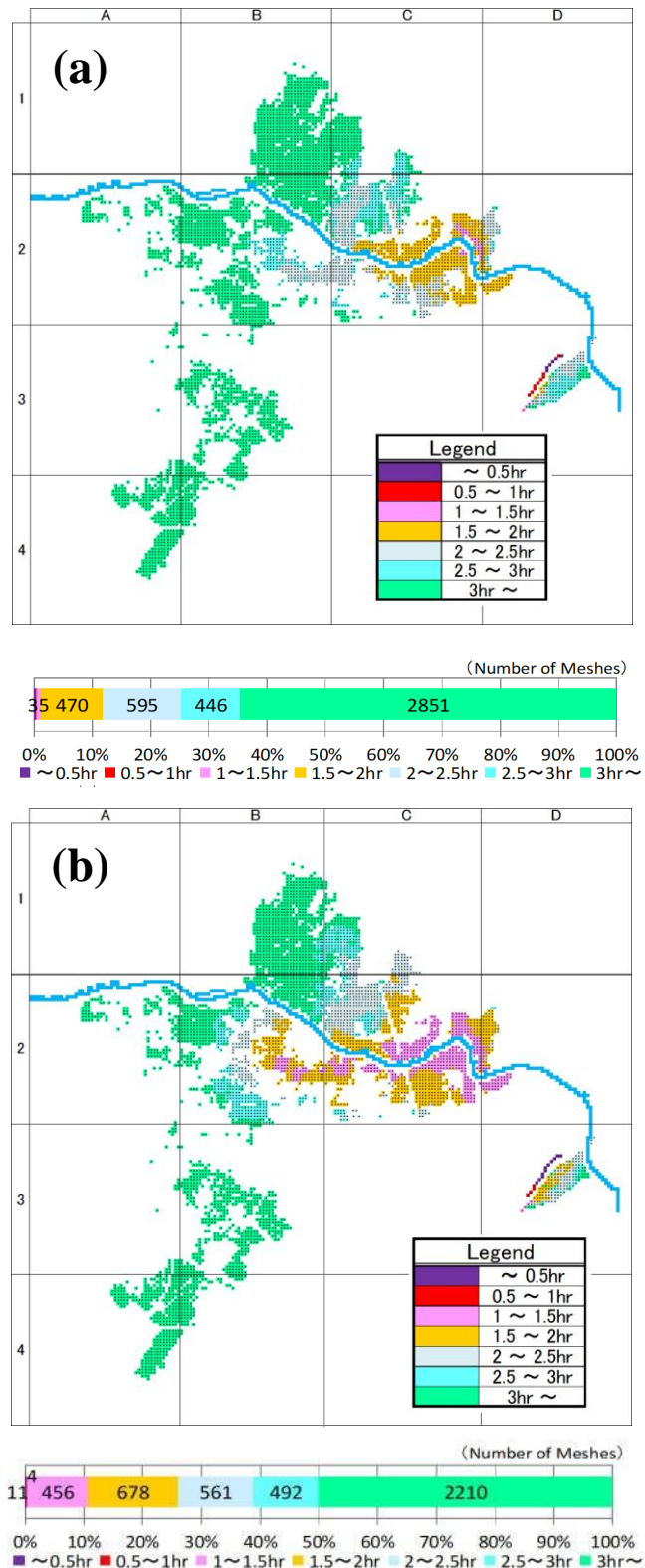


Figure 9 Potential Time of Evacuation (PTE) in condition of the alert level 3. (a) Evacuation by car. (b) Evacuation on foot.

other hand, PTE on foot shows increasing frequency of shorter evacuation time. These results indicate importance of considering the location of shelter and

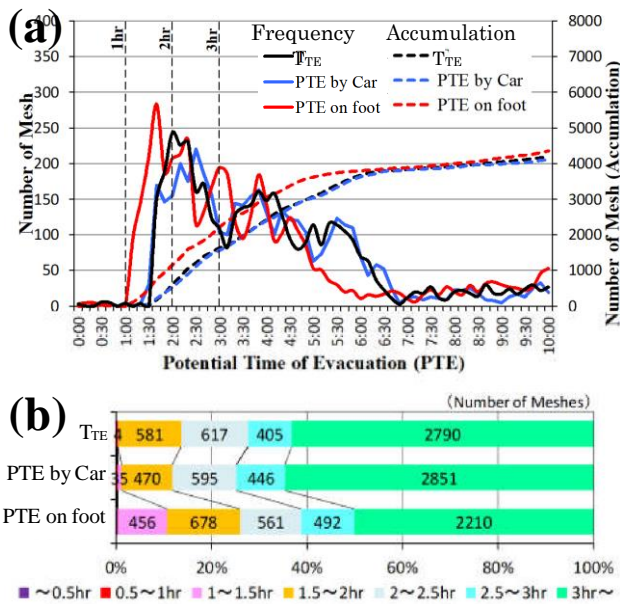


Figure 10 (a) Frequency distribution of PTE.
 (b) Stacked chart of T_{TE} and PTE. All results are for the alert level 3.

T_{TR} to perceive flood risk of each area appropriately.

Figure 11 is PTE estimated by using the alert level 4 criteria. The difference of T_{AL} between the alert level 3 and 4 (or 43 min) gives significant impact on the results. In some areas, PTE is shorter than 1 hr even in the case of evacuation by car. In the case of on foot, PTE is shorter than 1 hr in 10 % of the target grids. The shortest PTE is 40 min in on-foot evacuation. In such a case, there is quite small space for decision-making and announcement of evacuation directive by river administrator.

Figure 12a is frequency distribution of T_{TE} and PTE based on the alert level 4. Not negligible grids show $T_{TE} < 1hr$, and the results indicate emergent condition. Considering T_{TR} , the window time for evacuation (or PTE) is further shorter, and many people could come up against difficulty.

4. PTE estimation by different flood wave pattern

Using another flood wave pattern (the case of CNRM-CM5), PTE was calculated. Figure 13 shows a temporal variation of water level at Haneda. Water level reaches to the alert level 3 and 4 at 6:49, and

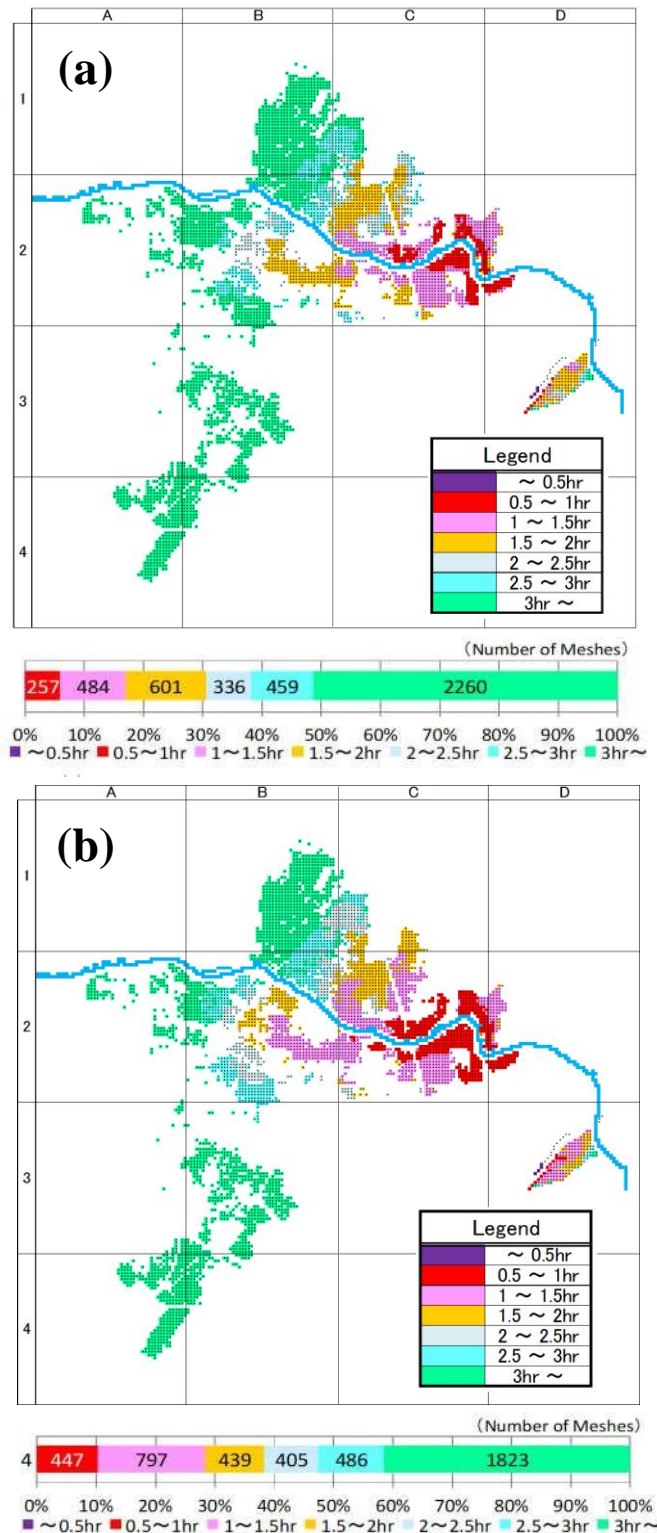


Figure 11 Potential Time of Evacuation (PTE) in condition of the alert level 4. (a) Evacuation by car. (b) Evacuation on foot.

7:14 on 29 July 2013, respectively. These times are used as T_{AL} to calculate PTE. Figure 14 shows spatial distribution of PTE. Because of higher peak discharge than the case of HadGEM2-ES, the

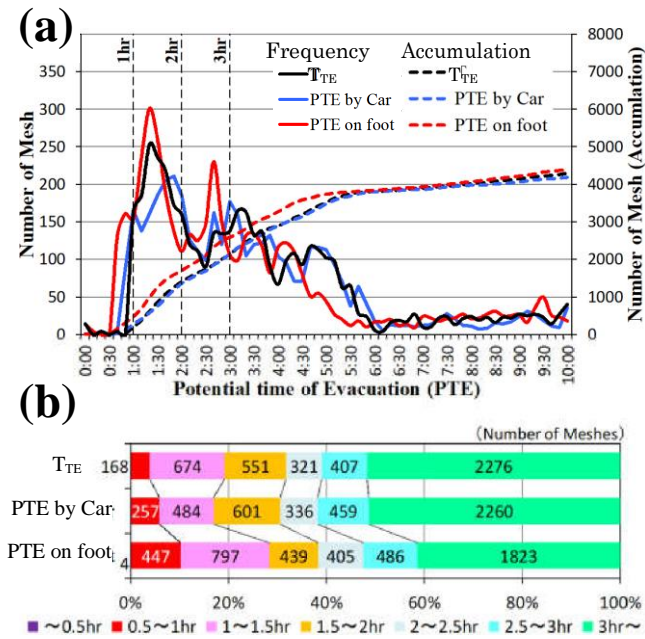


Figure 12 (a) Frequency distribution of PTE. (b) Stacked chart of T_{TE} and PTE. All results are for the alert level 4.

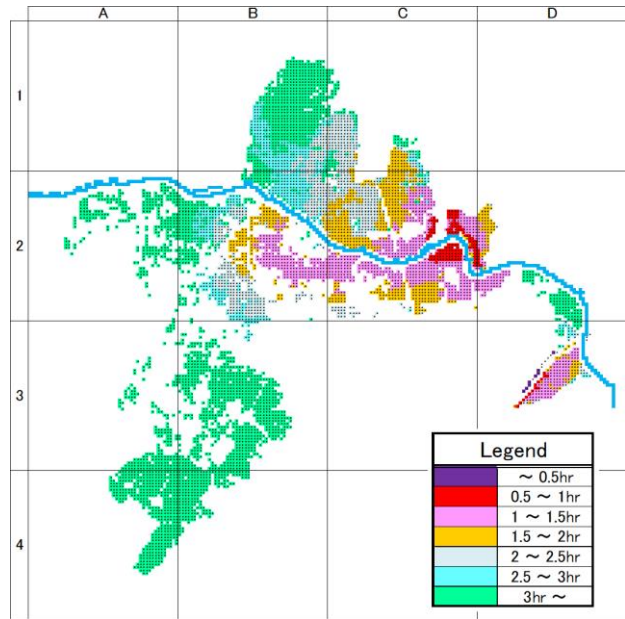


Figure 14 Potential Time of Evacuation (PTE) in the case of CNRM-CM5 (in condition of the alert level 3 for evacuation on foot).

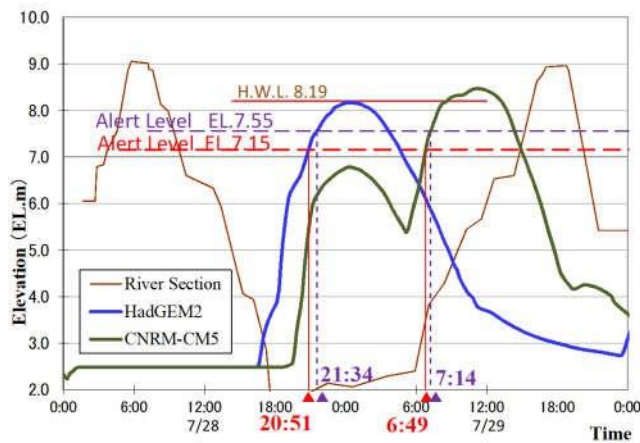


Figure 13 Temporal variation of water level at Haneda for the case of CNRM-CM5.

number of grid with inundation depth > 0.5m increased over 2,000. Spatial pattern of PTE is similar to that of HadGEM2-ES (Fig.9b), but the area with PTE < 1.5 hrs is about two times larger than HadGEM2-ES. At the same time, the area with PTE < 1 hr newly emerges in the result by CNRM-CM5. In the case of CNRM-CM5, the time difference between the alert level 3 and 4 is only 25 min. It indicates if decision-making and announcement of evacuation directive delays, the

condition gets worse in very short period. These results indicate importance of evaluation by using various patterns of flood waves.

5. Summary

To evaluate difficulty of evacuation under the heavy rainfall condition, potential time of evacuation (PTE) is calculated from the maximum window time of evacuation (T_{TE}), travel time to shelter (T_{TR}), and the time when water level reaches to alert level (T_{AL}) for Kakehasi river basin, Japan.

Results showed significant spatial dependency of PTE. In some computational grids, even the case of long T_{TE} , PTE is short because of far distance from shelters. Spatial distribution of PTE can bring a sense of urgency. People can properly perceive risk of inundation, and remaining time to start evacuation activity. At the same time, river administrators can recognize high-risk area and how long time remains to make an announcement for evacuation, or to start

flood prevention activity. Not only for real-time disaster prevention, but for making a timeline for emergency cases, PTE will be helpful information.

Two different flood wave patterns were used in this study. Inundation patterns and its temporal variations are affected by flood patterns. So multiple flood patterns have to be applied to consider various possibilities and uncertainties. At the same time, it is important to utilize updated results of global warming experiments.

In this study, effects of inland waters are not included. In the cases of heavy rainfall, inundation happens by inland waters before dyke breaks or overflow of river water, and it makes evacuation difficult. Therefore, effects of inland waters by heavy rainfall will be investigated in future works. At the same time, detail conditions of traffic networks and shelters under flood should be considered.

References

- 1) Kobayashi, S., Ota, Y., Harada, Y., Ebita, A., Moriya, M., et al., 2015. The JRA-55 reanalysis: General specifications and basic characteristics. *Journal of the Meteorological Society of Japan*, 93(1):5–48. doi:10.2151/jmsj.2015-001.
- 2) Ministry of Land, Infrastructure and Transport, Council for Social Infrastructure Report, 2018. *way of large-scale heavy rain measures ~ Emergency measures to prepare for complex disaster~*
- 3) Ministry of Land, Infrastructure and Transport, 2011. *Results of the research on tsunami damage in the Great East Japan Earthquake, Evacuation research results from tsunami*
- 4) National Centers for Environmental Prediction, National Weather Service, NOAA, U.S. Department of Commerce (2000). *NCEP FNL Operational Model Global Tropospheric Analyses, continuing from July 1999.* <https://rda.ucar.edu/datasets/ds083.2/#!docs>, Research Data Archive at the National Center for Atmospheric Research, Computational and Information Systems Laboratory. doi:10.5065/D6M043C6 (last date accessed: 27 Jul 2019).
- 5) Reynolds, R. W., Smith, T. M., Liu, C., Chelton, D. B., Casey, K. S., & Schlax, M. G., 2007. Daily high-resolution-blended analyses for sea surface temperature. *Journal of Climate*, 20(22): 5473–5496. doi: 10.1175/2007JCLI1824.1.
- 6) Sanuki, H., Shibuo, Y., Lee, S., Yoshimura, K., Tajima, Y., et al., 2016. Inundation forecast simulation in urbanized coastal low-lying areas considering multiple flood causing factors. *Japan Society of Civil Engineers, Ser. B2 (Coastal Engineering)*. 72(2): p. I_517-I_522.
- 7) Sato, T., Kimura, F., and Kitoh, A., 2007. Projection of global warming onto regional precipitation over Mongolia using a regional climate model. *Journal of Hydrology*, 333(1):144-154.
- 8) Sayama, T., Ozawa, G., Kawakami, T., Nabesaka, S., Fukami, K., 2012. Rainfall–runoff–inundation analysis of the 2010 Pakistan flood in the Kabul River basin. *Hydrological Sciences Journal*, 57(2): 298-312.
- 9) Skamarock, W. C., Klemp, J. B., Dudhia, J., Gill, D. O., Barker, J. M., et al., 2008, A description of the advanced research WRF version 3. NCAR Technical Note, NCAR/RN-475+STR. doi:10.5065/D68S4MVH.

- 10) Taylor, K. E., Stouffer, R. J., Meehl, G. A., 2012.
An overview of CMIP5 and the experiment
design. *Bull. Am. Meteorol. Soc.*, 93(4):485–498.
[doi.org:10.1175/BAMS-D-11-00094.1](https://doi.org/10.1175/BAMS-D-11-00094.1).